

# Velocity of vortex walls moved by current

P.-O. Jubert

IBM Research, Zurich Research Laboratory, CH-8803 Rüschlikon, Switzerland

M. Kläui

Fachbereich Physik, Universität Konstanz, Universitätsstrasse 10, D-78457 Konstanz, Germany, and IBM Research, Zurich Research Laboratory, CH-8803 Rüschlikon, Switzerland

A. Bischof

IBM Research, Zurich Research Laboratory, CH-8803 Rüschlikon, Switzerland

U. Rüdiger

Fachbereich Physik, Universität Konstanz, Universitätsstrasse 10, D-78457 Konstanz, Germany

R. Allenspach<sup>a)</sup>

IBM Research, Zurich Research Laboratory, CH-8803 Rüschlikon, Switzerland

Current-induced domain-wall motion experiments in 27 nm thick and 200–500 nm wide  $\text{Fe}_{20}\text{Ni}_{80}$  wires are reported. By imaging the domain-wall position after current injections, the mean wall velocities are determined. The initial velocity is found to be constant for pulse lengths between 2 and 25  $\mu\text{s}$  but decays after about ten injections. For samples with an increasing wire width the initial velocity is reduced.

Magnetic domain walls have recently become a focus of activity. Their static properties have been shown to differ significantly between the bulk and constrained thin-film geometries.<sup>1</sup> Furthermore, domain walls were successfully displaced in submicrometer wires, not only by applying magnetic fields but also by passing an electrical current through the wire.<sup>2–7</sup> This current-induced domain-wall motion opens up very interesting perspectives for using domain-wall manipulation in magnetic memory and logic devices.<sup>8</sup> The understanding of this effect, however, is still far from complete. A particularly interesting point is the interplay between the complex two-dimensional wall structure stabilized in these wires and the current, specifically, how the wall structure affects wall propagation and how the current pulse modifies the wall structure.

We addressed these points recently by combining magnetic imaging with current-induced domain-wall motion experiments.<sup>7</sup> We found a decay of the wall velocity after subsequent current injections. High-resolution imaging revealed that when a wall has become immobile its spin structure has been transformed from a vortex to a transverse configuration. This change in spin structure is directly correlated with the decay of the wall velocity.

Here we report an extension of these experiments to narrower and thicker wires. As in Ref. 7, we used a zigzag wire geometry, see Fig. 1(a). Straight wire segments are connected by bends that consist of ring sections, having a radius of 2  $\mu\text{m}$  and an angle of 45°. The bend-to-bend distance is 11.6  $\mu\text{m}$ . Wire widths varied from 200 to 500 nm. The structures were fabricated using electron-beam lithography and a two-step lift-off process, as described in Ref. 9. The substrate was a Si wafer covered by native oxide. 27 nm

$\text{Fe}_{20}\text{Ni}_{80}$  and a capping layer of 2 nm Au to prevent oxidation were deposited by molecular-beam epitaxy. The Au pads that provide an electrical contact to each wire were defined in an additional lithography step.

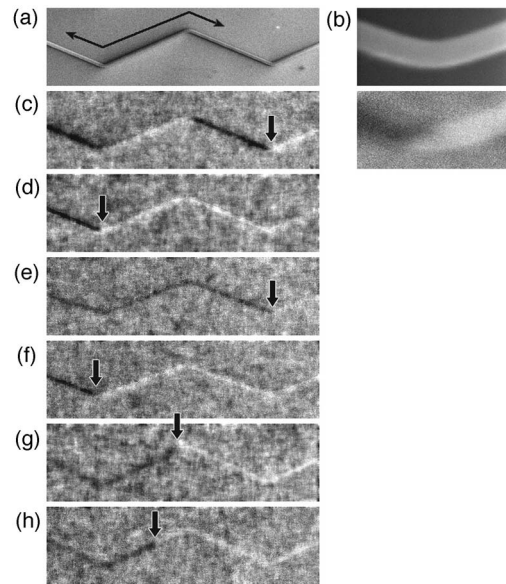


FIG. 1. (a) Topographic image of a  $\text{Fe}_{20}\text{Ni}_{80}$  wire with three bends. The wire ends (not shown) are connected to electrodes for wiring to the current source. (b) The close-up of the bend and its magnetic configuration after initially setting the state by a magnetic field. The wall exhibits a vortex. (c) Initial magnetic configuration after setting by a magnetic field. [(d)–(h)] Series of magnetization configurations in the wire. After image (c), a sequence of alternating current pulses of  $-2.4 \times 10^{12}$  and  $+2.4 \times 10^{12}$   $\text{A}/\text{m}^2$  of 25  $\mu\text{s}$  duration has been applied between the images, moving the wall across the bend to the left (negative current) or to the right (positive current). Subsequently, a positive pulse of 10  $\mu\text{s}$  has been injected resulting in image (g) and a negative pulse of 5  $\mu\text{s}$  before image (h). The arrows indicate the wall position.

<sup>a)</sup>Electronic mail: ral@zurich.ibm.com

The current-injection experiments and magnetic imaging were performed in our spin-polarized scanning electron microscope (spin-SEM) setup.<sup>10</sup> Topography and magnetization distribution are determined simultaneously. The capping layer was removed by a mild Ne<sup>+</sup> bombardment prior to imaging to reveal the Fe<sub>20</sub>Ni<sub>80</sub> surface.

The initial magnetic configuration of the zigzag wires can be controlled by an external magnetic field sweep. The resulting remanent state consists of domains of alternating magnetization directions in adjacent segments, see Fig. 1(c). At the bends head-to-head and tail-to-tail walls form.<sup>11</sup> The wire dimensions control the type of the domain walls.<sup>12</sup> All the wires investigated in this paper have equilibrium vortex walls. A typical image of such a wall is shown in Fig. 1(b).

The walls are moved by injection of current pulses with different pulse lengths, i.e., lasting between 2 and 25  $\mu$ s. In all experiments on the 300 nm wide sample reported here, the current density is kept constant at  $2.4 \times 10^{12}$  A/m<sup>2</sup>, slightly above the threshold current density of  $2.2 \times 10^{12}$  A/m<sup>2</sup>. A first negative current pulse of 25  $\mu$ s results in the configuration shown in Fig. 1(d). In our sign convention, a negative current corresponds to electrons flowing to the left in Fig. 1. Only one wall remains after the first injection: The wall at the right bend traveled to the left bend, whereas the other two walls were annihilated when they reached the left end of the wire. With successive positive and negative current pulses of 25  $\mu$ s duration, the remaining wall can be moved back and forth between the left and the right bend [Figs. 1(d)–1(f)]. A subsequent positive current pulse of 10  $\mu$ s positions the wall close to the center bend [Fig. 1(g)], while the next negative pulse of 5  $\mu$ s moves it halfway back [Fig. 1(h)]. With all injections we observe that the wall moves in the direction of the electron flow, confirming that a spin-torque effect<sup>13</sup> is responsible for the wall motion and not the Oersted field.

Figure 1 shows an interesting aspect of current-induced domain-wall motion which extends our earlier work. In Ref. 7 we made sure that the current-injection experiment was confined to the straight part of the wire. Figure 1 shows that this limitation is not necessary. Clearly, the bend is not an obstacle for the moving wall, in contrast to more severe wire-geometry variations such as a deep notch.<sup>14</sup> This is in line with our earlier observation that the threshold current densities for depinning a wall from the bend and from a position within the straight wire agree within the experimental accuracy of 10%.<sup>7</sup> We expect that the bend will only develop an effective pinning potential if the bend radius becomes comparable to the wall width or if the spin structure changes. For the geometry used here, the experimentally determined wall width is  $\approx 300$  nm and hence smaller than the bend radius by more than a factor of 6.

From the spin-SEM images as in Fig. 1, the wall position in the wire can be determined accurately after each current pulse. Thus a mean velocity can be derived, defined as the wall displacement between consecutive images divided by the current pulse width. Figure 2(a) presents the evolution of the wall velocities for the wall imaged in Fig. 1 as well as two other walls. For the first few injections, the velocity is rather constant before it decreases and eventually vanishes.

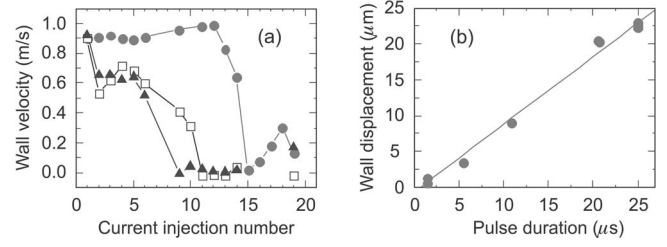


FIG. 2. (Color online) (a) Domain-wall velocity as a function of the number of current pulses, as determined from spin-SEM images, for three different walls (I, red circles; II, blue triangles; and III, black squares). The magnetic state was set by a magnetic field prior to pulse 1. After about 6–12 pulses, the velocity decreases and eventually vanishes. (b) Wall displacement vs pulse duration, determined from the first 12 current injections for wall I in (a). The straight line is a linear fit to the data, yielding a mean velocity of 0.94 m/s as a fit parameter.

We have already reported a similar “fatigue” effect for wider (500 vs 300 nm) and thinner (10 vs 27 nm) wires and have shown that the decay of the wall velocity is associated with a change in the wall structure from a vortex to a distorted transverse type.<sup>7</sup> We conclude that the observation of a wall velocity decaying with the number of current pulses is a general feature of the vortex walls in this geometry, but that the exact number of injections before the wall velocity decays varies.

Note that the predicted wall velocities in general are significantly higher<sup>15–17</sup> than those measured experimentally by us<sup>7</sup> and others.<sup>5</sup> From the theoretical model by Li and Zhang,<sup>18,19</sup> it is not even clear that the wall velocity stays constant during a current pulse. They find that the wall slows down owing to wall deformation within a nanosecond because the energy-damping rate increases with time.<sup>18</sup> More specifically, for a one-dimensional (1D) Néel wall the velocity completely disappears in the adiabatic limit.

Hence, a possible explanation for the observed small wall velocities could be that the walls only move during a short period at the beginning of the current pulse. Then our method of determining the mean velocity over the entire pulse duration by observing initial and final states would not be appropriate. We therefore varied the pulse duration from 2 to 25  $\mu$ s and determined the mean velocity for the first few injections for which the wall structure is still intact. A linear relation between wall displacement and pulse duration is found, see Fig. 2(b). This linearity demonstrates that the walls move on a time scale of microseconds rather than nanoseconds, and at least on this time scale the velocity is constant. We cannot exclude that the prediction of a larger velocity in the first nanosecond is correct, as our experimental setup does not yet allow us to inject pulses of nanosecond duration.

The dependence of velocity on geometry is discussed next. Comparing the velocities for different samples, we find significant differences for the initial wall velocity  $v$ :  $v=0.9$  m/s for 300 nm wide and 27 nm thick wires, whereas  $v=0.3$  m/s for 500 nm wide and 10 nm thick wires. For 27 nm thick structures, we have systematically varied the wire width and determined the initial wall velocities, as presented in Fig. 3. The ratio of current density to threshold current density has been kept between 1.03 and 1.10. The

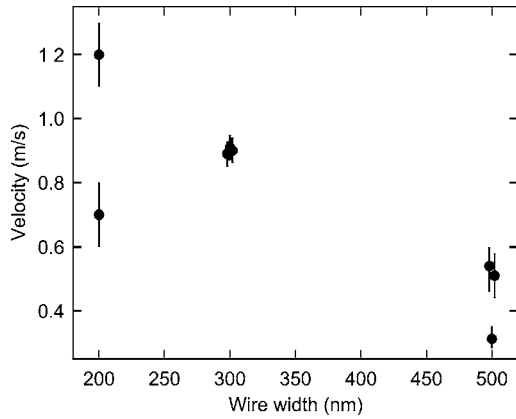


FIG. 3. Domain-wall velocity as a function of the wire width for a constant wire thickness of 27 nm. The ratio of current density to threshold current density is kept between 1.03 and 1.10. The error bars indicate the inaccuracy in wall position determination.

changes of wall velocity with varying wire dimensions are again observed. Despite a (yet) small number of experimental points, the general trend is that the velocity decreases with an increasing wire width. This is not expected from an adiabatic spin-transfer model,<sup>20</sup> in which—for a constant ratio of current to threshold current—the velocity is proportional to the perpendicular anisotropy, which increases for an increasing wire width. The observation that the wall velocity depends on the geometry also disagrees with the theoretical models by Li and Zhang<sup>18</sup> and by Thiaville *et al.*<sup>17</sup> In these 1D models the velocity is independent of the wall width, which implicitly depends on the geometry at submicrometer dimensions. More detailed experiments are needed to investigate whether the two-dimensional (2D) spin structure of the walls is responsible for the observed geometry-dependent velocities.

In conclusion, we have investigated current-induced domain-wall motion along  $\text{Fe}_{20}\text{Ni}_{80}$  wires of 300 nm in width and 27 nm in thickness in detail. We find that, for the first current injections, the walls move with largely unchanged velocity in straight wires and around bends for pulses between 2 and 25  $\mu\text{s}$ . On the other hand, as in our earlier investigation on wider and thinner wires, after a number of current injections the vortex wall velocity decreases

and eventually the wall stops. The velocity is found to depend on wire geometry, with the trend of wider wires exhibiting smaller velocities. Both results cannot be explained with recent theoretical predictions. We expect that the extension to 2D domain-wall models similar to Ref. 17 and further theoretical development including nonadiabatic effects will lead to a better agreement between theory and experiment.

The authors acknowledge C. A. F. Vaz, J. A. C. Bland, G. Faini, L. Vila, C. Vouille, and M. Witzig for sample fabrication. One of the authors (M.K.) would like to thank the “Deutscher Akademischer Austauschdienst” (DAAD) and the DFG (SFB 513) for financial support.

- <sup>1</sup>P.-O. Jubert, R. Allenspach, and A. Bischof, *Phys. Rev. B* **69**, 220410R (2004).
- <sup>2</sup>J. Grollier, P. Boulenc, V. Cros, A. Hamzić, A. Vaurès, A. Fert, and G. Faini, *Appl. Phys. Lett.* **83**, 509 (2003).
- <sup>3</sup>M. Tsoi, R. E. Fontana, and S. S. P. Parkin, *Appl. Phys. Lett.* **83**, 2617 (2003).
- <sup>4</sup>N. Vernier, D. A. Allwood, D. Atkinson, M. D. Cooke, and R. P. Cowburn, *Europhys. Lett.* **65**, 526 (2004).
- <sup>5</sup>A. Yamaguchi, T. Ono, S. Nasu, K. Miyake, K. Mibu, and T. Shinjo, *Phys. Rev. Lett.* **92**, 077205 (2004).
- <sup>6</sup>M. Kläui, C. A. F. Vaz, J. A. C. Bland, W. Wernsdorfer, G. Faini, E. Cambril, and L. J. Heyderman, *Appl. Phys. Lett.* **83**, 105 (2003).
- <sup>7</sup>M. Kläui *et al.*, *Phys. Rev. Lett.* **95**, 026601 (2005).
- <sup>8</sup>D. A. Allwood, G. Xiong, M. D. Cooke, C. C. Faulkner, D. Atkinson, N. Vernier, and R. P. Cowburn, *Science* **296**, 2003 (2002).
- <sup>9</sup>M. Kläui, C. A. F. Vaz, J. A. C. Bland, W. Wernsdorfer, G. Faini, and E. Cambril, *Appl. Phys. Lett.* **81**, 108 (2002).
- <sup>10</sup>R. Allenspach, *J. Magn. Magn. Mater.* **129**, 160 (1994).
- <sup>11</sup>T. Taniyama, I. Nakatani, T. Namikawa, and Y. Yamazaki, *Phys. Rev. Lett.* **82**, 2780 (1999).
- <sup>12</sup>R. D. McMichael and M. J. Donahue, *IEEE Trans. Magn.* **33**, 4167 (1997).
- <sup>13</sup>L. Berger, *J. Appl. Phys.* **55**, 1954 (1984).
- <sup>14</sup>M. Kläui, C. A. F. Vaz, J. A. C. Bland, W. Wernsdorfer, G. Faini, E. Cambril, L. J. Heyderman, F. Nolting, and U. Rüdiger, *Phys. Rev. Lett.* **94**, 106601 (2005).
- <sup>15</sup>S. Zhang and Z. Li, *Phys. Rev. Lett.* **93**, 127204 (2004).
- <sup>16</sup>A. Thiaville, Y. Nakatani, J. Miltat, and N. Vernier, *J. Appl. Phys.* **95**, 7049 (2004).
- <sup>17</sup>A. Thiaville, Y. Nakatani, J. Miltat, and Y. Suzuki, *Europhys. Lett.* **69**, 990 (2005).
- <sup>18</sup>Z. Li and S. Zhang, *Phys. Rev. Lett.* **92**, 207203 (2004).
- <sup>19</sup>Z. Li and S. Zhang, *Phys. Rev. B* **70**, 024417 (2004).
- <sup>20</sup>G. Tatara and H. Kohno, *Phys. Rev. Lett.* **92**, 086601 (2004).